J Mater Cycles Waste Manag (2010) 12:10–16
DOI 10.1007/s10163-009-0267-z

SPECIAL FEATURE: ORIGINAL ARTICLE

Special Feature on APLAS Sapporo 2008

Jun Kobayashi · Katsuya Kawamoto

Catalyst durability in steam reforming of thermally decomposed waste wood

Received: September 29, 2008 / Accepted: September 14, 2009

Abstract Thermal gasification and reforming technologies applicable over a wide temperature range were investigated for high efficiency and for the calorific value of the gas evolved from organic waste such as woody debris. The durability of the reforming catalyst and the availability of catalyst regeneration were investigated using laboratory-scale catalytic reformers and a gasifier. Commercial Ni-based catalyst and calcined limestone (CaO) were applied to the reforming reaction. The results of woody waste gasification and reforming revealed the hydrogen concentration produced to be sustained at a high catalyst temperature of 1123 K, which prevented the catalyst from deactivating. The results also indicated that catalyst regeneration by air oxidation at the same temperature would be effective for enhancing catalytic activity.

Key words Gasification · Waste wood · Reforming · Nickel catalyst · Hydrogen

Introduction

Flammable waste such as waste biomass, municipal solid waste, and waste plastics are regarded as an energy resource because their calorific value is of the order of tens of megajoules per kilogram. Currently, there are over 1000 waste incineration facilities in Japan, and more than 20% of these facilities include electricity-generating processes. It has been suggested that expanding the use of flammable waste would contribute to reducing greenhouse gas emissions and fossil fuel consumption. Although steam turbine generation is most commonly used, its power generation efficiency is around 20% or less. Corrosion of the heat exchanger and the relatively low calorific value of the waste are the major causes of this low efficiency when burning flammable waste; fossil fuel contains few corrosive compounds and has a much larger calorific value. Therefore, the combustion temperature of the fossil fuel is often much higher than that of flammable waste. On the other hand, conversion of such waste to fuel gases (the gasification process) can lead to highly efficient power generation because the fuel gases can be applied to a gas turbine or fuel cell for power generation. To achieve practical use of the gasification process, however, it is necessary to optimize the fuel characteristics such as the composition and heating value of the gases. Moreover, issues affecting the power generation performance, such as tar and corrosive compounds in the gases, as well as the energy efficiency, must be addressed. There is, therefore, a pressing need to improve the gasification process. Many kinds of gasifiers, such as fluidized-bed,[1,2] entrained-bed,[3] and rotary-kiln[4] gasifiers have been proposed, and extensive research studies and experiments are being conducted. Our studies have focused on steam gasification and reforming of waste biomass using a reforming catalyst.[5]

The chief aim of biomass gasification using steam reforming reactions is to synthesize hydrogen-rich gas. The ideal hydrogen composition in synthesis gas is determined by reaction equilibria, but the actual composition would be influenced by the overall reaction rate. This overall reaction rate is related to the absolute reaction rate and to mass and heat transfer, and these in turn depend on the reaction conditions such as temperature, pressure, and concentration of gasifying agents. The absolute reaction rate usually increases with an increase in the reaction temperature, regardless of the equilibrium. On the other hand, by using reforming catalysts in the process, the absolute reaction rate would increase even if the temperature were relatively low. In recent reports on the application of reforming catalysts to biomass gasification, different catalysts have been proposed, and noble metals such as Pt, Rh, and Pd[6,7] and base metals such as Ni and Co[8] have been evaluated. Moreover, catalytic supports such as alumina, silica, ceria (CeO_2), and alkaline earth metal compounds have been investigated. Thus, steam reforming of hydrocarbons, which contain tar, methane, and ethylene, among others, must be improved for development of hydrogen production destined for fuel cell power generation.

J. Kobayashi (✉) · K. Kawamoto
National Institute for Environmental Studies, 16-2 Onogawa, Tsukuba, Ibaraki 305-8506, Japan
Tel. +81-29-850-2061; Fax +81-29-850-2091
e-mail: jkoba@nies.go.jp

Nickel catalysts usually exhibit high catalytic performance when promoting hydrogen conversion from biomass. Nickel is also relatively easy to procure compared to rare metals and rare earths, making it cheaper than these materials. This prompted us to select Ni as the reforming catalyst in this study. The major problem with Ni catalysts is deactivation due to carbon deposition on the catalyst surface (coking) and poisoning by H_2S.[9–11] Maintaining long-term catalytic activity is therefore an important issue. In response, extensive investigations have been conducted on alkali metal compounds such as CaO and MgO, as well as on natural minerals such as dolomite and olivine.[12–14]

The purpose of this study was to evaluate the durability of a commercial Ni reforming catalyst and the effect of additive CaO on the reforming behavior, and to clarify in detail the factors that affect catalytic performance and the effect of operating parameters on the characteristics of produced gas composition. The catalyst was developed not for biomass gasification but for the steam reforming of petrochemical feedstocks. However, we predicted that this catalyst could actively decompose tar because it includes CaO in the Al_2O_3 support. Moreover, the effect of the combination of the catalyst and CaO on biomass gasification has not been clarified. In addition, regeneration of the catalyst by air oxidation, i.e., the removal of deposited carbon, was also carried out and the behavior of catalytic activity based on gas composition and material properties such as the crystal structure was investigated.

Experimental

Apparatus

A laboratory-scale gasification unit was built to conduct the experiments, as shown in the schematic representation in Fig. 1. The system essentially consists of two kinds of reactors in series: a primary reactor (gasifier) followed by two secondary reactors (reformers) made of stainless steel. The primary reactor was a fluidized-bed type [internal diameter (ID) 37–50 mm, height (H) 1360 mm], and the secondary reactors were packed-bed types (ID 48 mm, H 1620 mm), both preheated by electric heaters. Three thermocouples were placed in the gasifier at distances of 50, 350, and 650 mm above the distributor to measure the temperature of the fluidized bed, the internally circulating particles, and the area near the outlet, respectively. Additionally, two thermocouples were installed in the reformers, one buried in the catalyst bed and the other placed about 50 mm below the catalyst bed, to determine the temperature of the reforming zone and the reformed gas, respectively.

In this system, feedstock is supplied from the upper part of the gasifier and silica sand is used as the fluidized bed material in the gasifier. To carry out the reforming process and catalyst regeneration simultaneously, two reformers are connected to the gasifier through several valves that are used for switching between reforming and regeneration. All pipelines are kept at around 573 K by using insulating jackets. As the oxidizing agent, steam and simulated air (mixed nitrogen and oxygen) are preheated to around 550–600 K and the mixture is supplied from the bottom of the gasifier. When the gaseous mixture passes through the distributor, the feedstock and silica sand are fluidized and mixed in the gasifier. This is constantly heated by the electric heater, since the thermal decomposition and volatilization of the feedstock are endothermic. The produced gases and tar in the gasifier pass through the cyclone, where unreacted char and fly ash are removed, and then move on to the reformer. The tar and low hydrocarbons are reformed by steam on the surface of the reforming catalyst and are converted into gases such as H_2, CO, and CO_2.

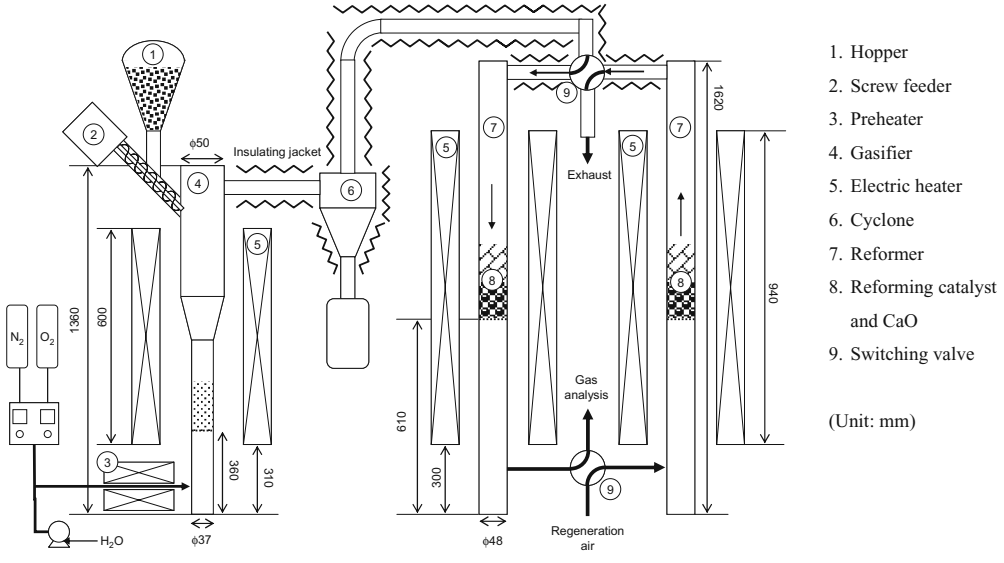

Fig. 1. Schematic of the experimental apparatus. *1*, Hopper; *2*, screw feeder; *3*, preheater; *4*, gasifier; *5*, electric heater; *6*, cyclone; *7*, reformer; *8*, reforming catalyst and CaO; *9*, switching valve. All dimensions are in millimeters

Table 1. Proximate and ultimate analysis of feedstock

Volatile (wt% dry)	80.0	H (wt% dry)	5.9
Fixed carbon (wt% dry)	18.0	C (wt% dry)	51.4
Ash (wt% dry)	2.0	O (wt% dry)	40.7
Moisture (wt%)	9.0	N (wt% dry)	<0.1
HHV (MJ/kg dry)	20.5	Cl (wt% dry)	<0.01
LHV (MJ/kg dry)	17.2	S (wt% dry)	<0.02

HHV, higher heating value; LHV, lower heating value

Table 2. Ultimate analysis of ash in feedstock

Al (wt% dry)	3.1	Cd (mg/kg dry)	<5
Ca (wt% dry)	4.9	Pb (mg/kg dry)	58
Fe (wt% dry)	6.3	As (mg/kg dry)	21
Si (wt% dry)	12.6	Cr (mg/kg dry)	16
Na (wt% dry)	2.5	Cu (mg/kg dry)	200
Se (mg/kg dry)	<5	Hg (mg/kg dry)	<0.05

Table 3. Experimental conditions

Run number	1	2	3
Feed rate (kg/h)	0.18	0.17	0.20
Gasifier temp. (K)	1123	1123	1123
First reformer temp. (K)	1123	1123	1123
Second reformer temp. (K)	1073	1123	1023
S/C (mol/mol)	2.1	2.6	1.8
ER (–)	0.12	0.16	0.12
First reformer			
CaO (g)	106.7	0	105.8
Catalyst (g)	99.7	50.1	50.6
Second reformer			
CaO (g)	98.2	0	106.4
Catalyst (g)	99.5	50.8	50
Space velocity (h^{-1})	7800	18000	15000

Temp., temperature; S/C, ratio of steam/carbon in the feedstock; ER, equivalence ratio for oxygen

Feedstock and reforming catalyst

In this study, construction and demolition woody waste was pulverized to produce 1–2 mm particles for use as feedstock. Proximate and ultimate analyses of the feedstock and its ash are shown in Tables 1 and 2. Since the woody waste had been treated with preservatives and insecticides, it contained heavy metals such as Cu, Cr, and As (CCA). On the other hand, the ash content was low and that of volatile matter was very high. Moreover, the feedstock contained more than 40 wt% oxygen due to the presence of cellulose and xylose.

Ni-based commercial reforming catalyst (Süd-Chemie Catalysts Japan) was used in the experiments. This catalyst was originally developed for petrochemical refining and has demonstrated excellent performance in promoting organic matter reform without reduction treatment. This catalyst contains Ni at 11 wt% and CaO at 13 wt%, with the balance being Al_2O_3. The catalyst was supplied in the form of a ten-holed ring with a diameter of 19 mm and height of 16 mm. The catalyst was pulverized and classified into pieces 2–5 mm in diameter for use in the experiments. CaO particles of calcined limestone (Niimi Chemical Industries) were used with the catalyst to assist tar decomposition, the removal of CO_2 by chemical sorption, or both. The particle size was almost the same as that of the catalyst.

Procedure

The experimental conditions in this study are shown in Table 3. After the gasifier and reformers had been preheated and maintained at the desired temperature for several hours, feedstock was sequentially supplied to the gasifier from the hopper through a screw feeder with air and steam. Gas produced from the gasifier was introduced into each reformer and one was used for the reforming reaction for about 1 h. The other was used to regenerate the catalyst by using air at 3 l/min at the same time to remove tar, carbon deposits, or both on the catalyst surface due to coking. The regeneration period was about 30 min, after which the air in the reformer was purged with nitrogen. The gas line was then switched from reforming to regeneration. The gas produced was introduced into scrubbing bottles placed in an ice bath. Tar and steam were condensed and deposited in the bottles. After the tar had been removed, the gas was passed through a series of gas analyzers: H_2, O_2, N_2, CO, CH_4, C_2H_2, C_2H_4, and C_2H_6 were analyzed every 5 min using a Micro-GC 3000 (Agilent Technologies). CO_2 and total hydrocarbons were also sequentially determined using a GC 7000 series (Shimadzu) and EHF 770 (Yanaco), respectively.

The amount of steam injection was expressed as the ratio of steam/carbon in the feedstock (S/C, mol/mol), while oxygen was expressed as the equivalence ratio (ER), the ratio of actual/theoretical amount of oxygen. Since the feed rate fluctuated even when the rotation speed of the screw was kept constant, the feed rate (designated as 0.18 kg/h) was calculated after the experiments according to the amount of feedstock actually supplied. This caused fluctuations in the experimental results such as changes in the composition of the gas produced.

Results and discussion

Gas composition

The results of run 1 are shown in Figs. 2–5. Here, Figs. 2 and 4 show changes in the composition of the gas produced through the first reformer, and Figs. 3 and 5 show changes through the second reformer. Moreover, the regeneration period between cycles 2 and 3 for the first reformer was more than 1 h, although the period for the others was about 30 min.

As shown in Figs. 2 and 3, hydrogen concentration was almost constant for every cycle, except for the first cycle of each reformer. Comparing cycles 2 and 3 in Fig. 2, however, the hydrogen concentration in the third cycle was greater than that in the second cycle, at around 60 vol%. The range of hydrogen concentration in the others was mostly 50–55 vol%. The concentration of carbon dioxide was rela-

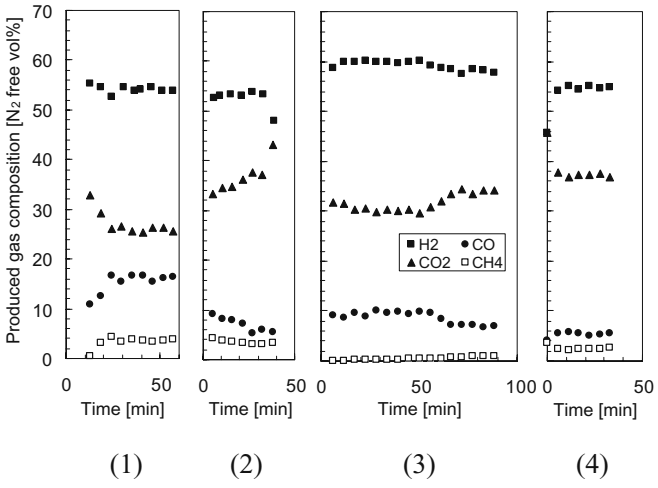

Fig. 2. Changes in produced inorganic gas composition with time (run 1, first reformer). *Numbers* in parentheses represent the cycle number

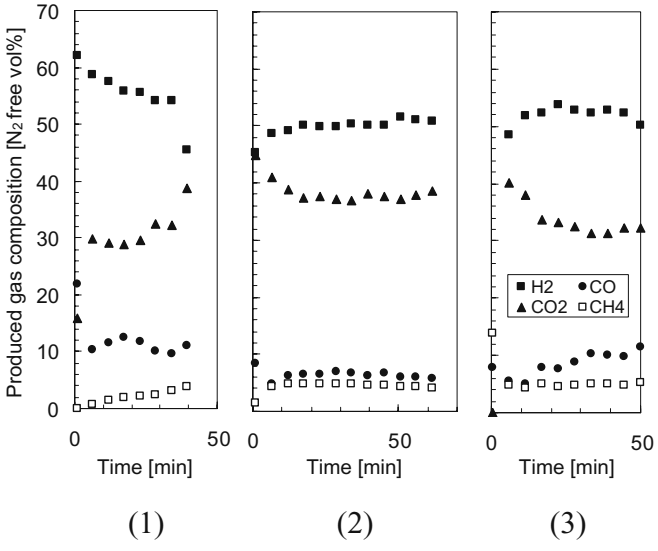

Fig. 3. Changes in produced inorganic gas composition with time (run 1, second reformer)

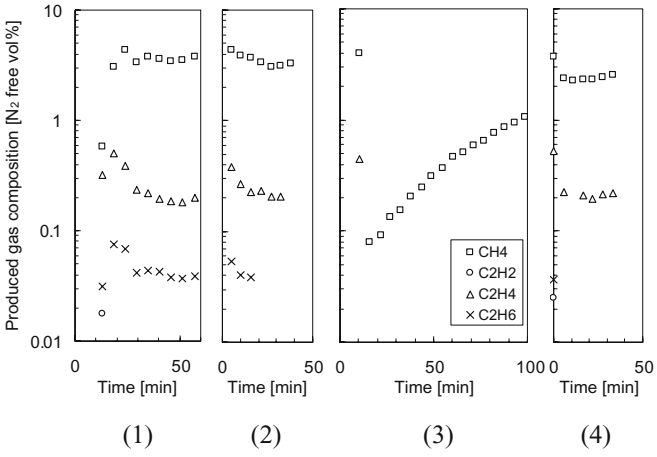

Fig. 4. Changes in produced hydrocarbon composition with time (run 1, first reformer)

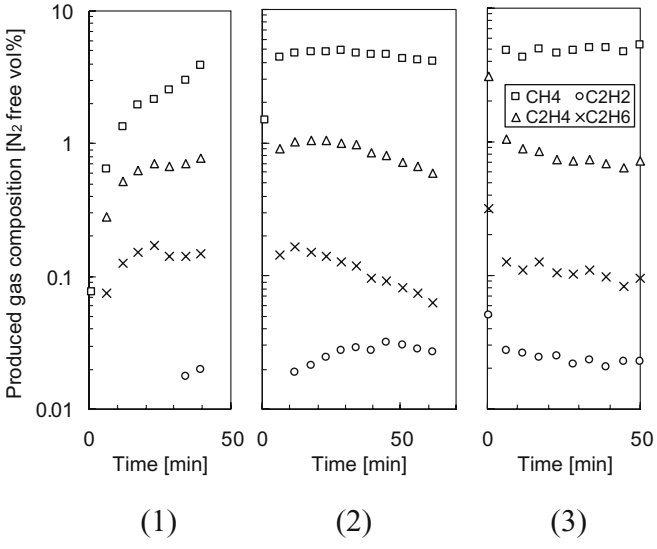

Fig. 5. Changes in produced hydrocarbon composition with time (run 1, second reformer)

tively high (30 vol%–35 vol%) and that of carbon monoxide was relatively low (below 10 vol%, except for the first cycle). From Figs. 4 and 5, a distinctive change in hydrocarbon concentration was indicated in the third cycle of the first reformer, and few hydrocarbons other than C_2 were detected. The methane concentration during the third cycle was much lower than that in the others, but it gradually increased with time. In the fourth cycle of the first reformer, the concentration of methane and ethylene was almost constant and was similar to those of the first and second cycles, but no ethane was detected. In contrast, the concentration of methane and ethylene increased with time in the first cycle of the second reformer and was almost constant in the later cycles. Moreover, the composition of methane and ethylene in the second reformer was usually greater than that at the first reformer, and acetylene was contained in the gas produced using the second reformer. Since the reforming temperature of the second reformer was slightly lower than that of the first reformer, the reaction rate of the thermal decomposition of hydrocarbons was lower in the second reformer.

The results of run 2 are shown in Figs. 6 and 7. Here, both figures show the composition of the gas produced using the first reformer. Since the results for the second reformer were almost the same as those for the first reformer, their details are omitted.

The hydrogen concentration gradually decreased with time for each cycle except for the first cycle, and the average concentration for each cycle also decreased with repeated regeneration. The fluctuation range of hydrogen concentration was close to 50–58 vol%. Regarding hydrogen concentration, the concentration of hydrocarbons increased with time for every cycle and by repeated regeneration. In comparison with the results of run 1 using the first reformer, the concentration of hydrocarbons and carbon monoxide was high overall.

The results of run 3 for the first and second reformers are shown in Figs. 8 and 9, respectively. Here, both figures

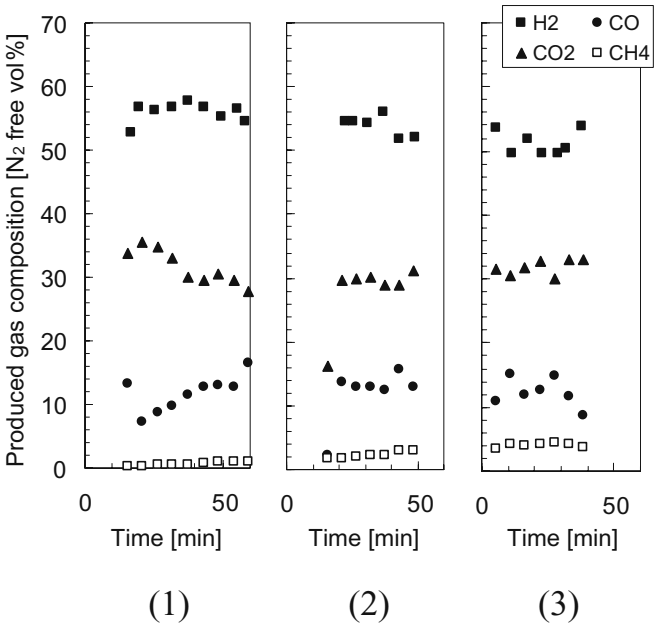

Fig. 6. Changes in produced inorganic gas composition with time (run 2, first reformer)

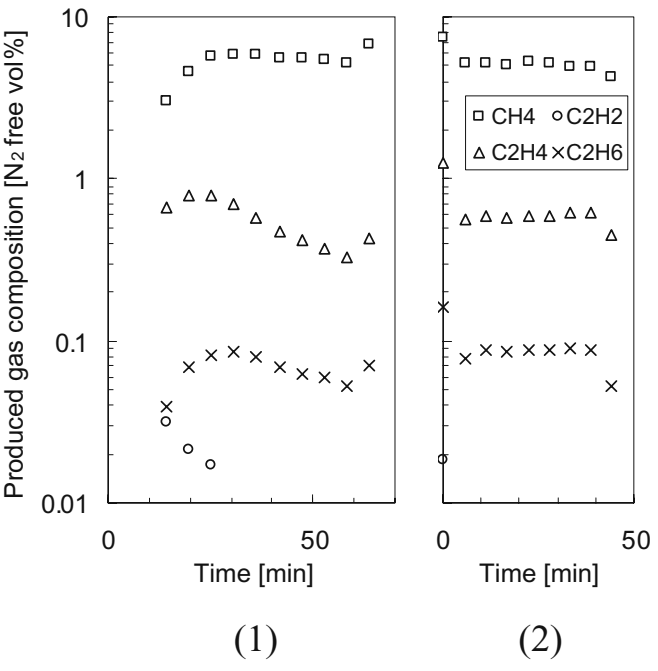

Fig. 8. Changes in produced hydrocarbon composition with time (run 3, first reformer)

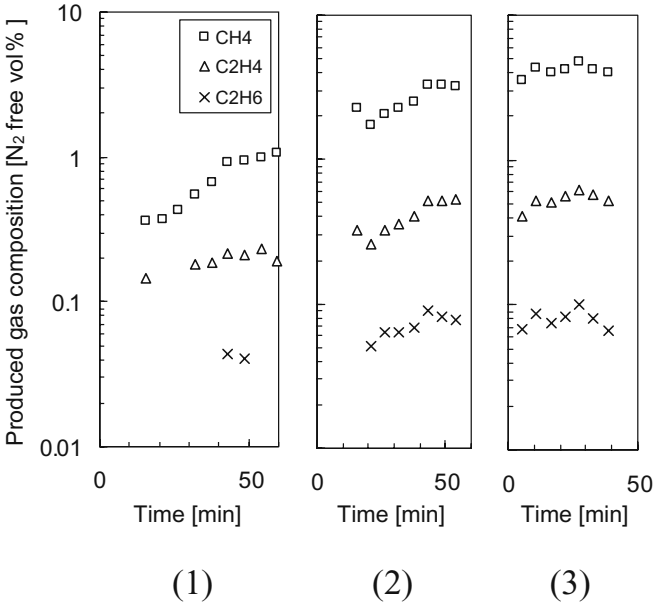

Fig. 7. Changes in produced hydrocarbon composition with time (run 2, first reformer)

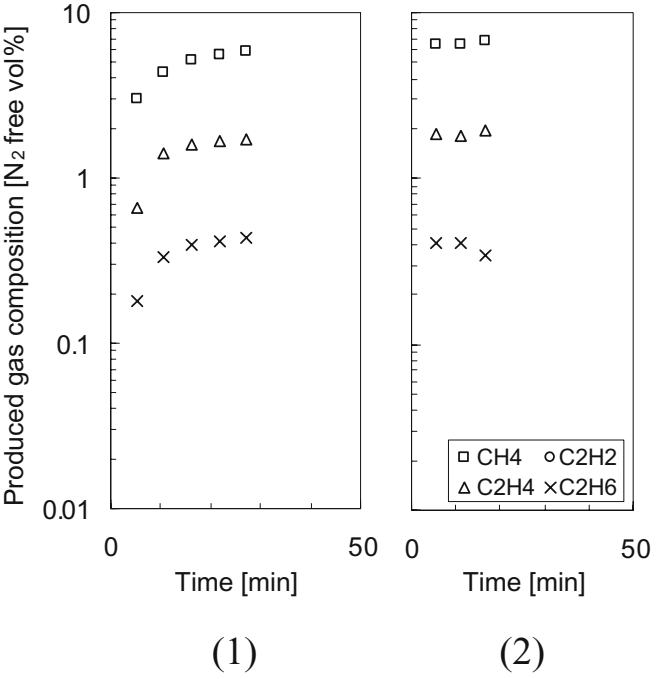

Fig. 9. Changes in produced hydrocarbon composition with time (run 3, second reformer)

indicate the produced hydrocarbon composition, since the results were distinctive. The methane concentration for each reformer was not significantly different, but the ethylene and ethane concentration in the second reformer was much higher than that in the first reformer. In addition, these concentrations showed little difference between the end of the first cycle and the beginning of the second cycle for both reformers.

The above-mentioned results indicate that catalyst activity with CaO was more or less maintained at a reforming temperature of 1123 K, since the concentration of hydrogen and hydrocarbons was virtually constant for each cycle despite the very large space velocity of the catalyst bed. In addition, the hydrogen concentration under the above-mentioned conditions was almost the same as the equilibrium concentration (57 N_2-free vol%). Therefore, these

conditions could result in higher catalyst durability than the other conditions. Moreover, the results indicate the possibility of improving the regeneration of the reforming catalyst by optimizing the air oxidation treatment, especially the oxidation period and temperature, since catalyst activity in the third cycle was much higher than that in the second cycle in run 1. However, the mechanism of reactivation of the catalyst, especially the third cycle of run 1 using the first reformer, is not clear, making it necessary to give in-depth consideration to the regeneration conditions. It was also found that catalytic activity for reforming hydrocarbons proportionally decreased with a decline in the reforming temperature to below 1123 K, even if CaO was used. The decomposition reaction of tar, hydrocarbons, or both at high temperatures was accelerated by the presence of CaO.

Hydrogen production and HHV

Tables 4–6 show the mean higher heating value (HHV) per unit volume and the amount of produced hydrogen per unit mass of feedstock, as calculated from the gas composition of each experimental result. The mean value of hydrogen production covered about 40–50 mol/kg-feedstock rounded to the nearest ten, except for the case of the third cycle in run 1 using the first reformer. When applying CaO at a reformer temperature of 1123 K, hydrogen production was mostly maintained despite repeated regeneration. For the other conditions, however, the greater the number of regeneration operations, the greater the decrease in hydrogen production, especially at relatively low reformer temperatures. The gas produced had a mean HHV in the range of 6–10 MJ/m_N^3. There was no clear relationship between HHV and the experimental conditions. From the results of hydrogen production, it was also clarified that catalyst activity with CaO was roughly maintained at a reforming temperature of 1123 K.

The compositions and heating values of the produced gases suggest that they have potential for application to power generation processes. Since the produced gas had a heating value higher than 4.2 MJ/m_N^3, it is usable in gas engines. The power generation efficiency of recent gas engines is around 30% or more. The power generation efficiency based on input waste energy will thus exceed 20% if the cold gas efficiency is more than 70%. Moreover, generation efficiency could exceed 30% if the produced gas is fed into a solid oxide fuel cell (SOFC), because the gas is primarily composed of H_2 and CO. Since these experiments were carried out using a high-powered electric furnace to ensure temperature stability, it was difficult to evaluate the cold gas efficiency. However, a cold gas efficiency of 70% would be achievable if the design were optimized and scaled up.

X-ray diffraction analysis of the catalyst

Figure 10 shows the results of X-ray diffraction (XRD) analysis of the catalyst used in run No. 1 as well as analysis of the fresh catalyst. Metallic nickel crystal growth occurred even under repeated catalyst regeneration by air oxidation. For the fresh catalyst, on the other hand, only peaks caused by $CaAl_4O_7$ (grossite) and Al_2O_3 were confirmed, with no peaks of metallic nickel.

It is difficult to detect metallic nickel in the fresh catalyst, since it contains nanometer-sized active sites in the form of nanoparticle nickel. The crystal growth of metallic nickel indicates the sintering of nanoparticle nickel, but reduced catalytic activity due to such sintering was not confirmed from the results of run 1. It thus appears that the sintered active sites could be separated by repeated reduction by the gas from the gasifier after air oxidation. For this reason, the nanometer-sized active nickel sites could be rebuilt and catalytic activity could be maintained. To clarify the relationship between crystal structure and activity, investigations based on further microscopic observations are necessary.

Table 4. Average hydrogen production per unit mass of feedstock and HHV of the gas produced in run 1

Run 1	Average H_2 produced (mol/kg-feedstock)	Average HHV (MJ/m_N^3)
First reformer		
First cycle	46	9.6
Second cycle	44	7.1
Third cycle	56	7.7
Fourth cycle	47	6.6
Second reformer		
First cycle	49	8.7
Second cycle	38	7.2
Fourth cycle	42	8.3

Table 5. Average hydrogen production per unit mass of feedstock and HHV of produced gas for run 2

Run 2	Average H_2 produced (mol/kg-feedstock)	Average HHV (MJ/m_N^3)
First reformer		
First cycle	50	7.3
Second cycle	45	8.4
Third cycle	40	8.2
Second reformer		
First cycle	52	8.1
Second cycle	40	8.2

Table 6. Average hydrogen production per unit mass of feedstock and HHV of produced gas for run 3

Run 3	Average H_2 produced (mol/kg-feedstock)	Average HHV (MJ/m_N^3)
First reformer		
First cycle	46	9.6
Second cycle	44	7.1
Second reformer		
First cycle	49	8.7
Second cycle	38	7.2

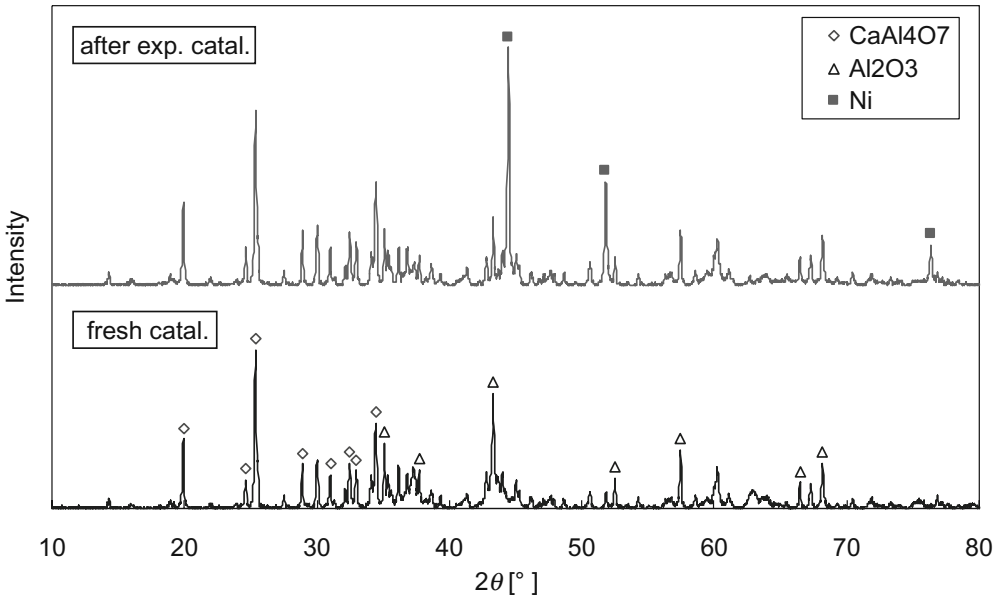

Fig. 10. X-ray diffraction patterns for used and fresh catalyst (run 1, first reformer)

Conclusions

Biomass gasification using nickel catalyst under various conditions was carried out to clarify the durability of the catalyst and the effect of the regeneration process on catalytic activity. The following conclusions were drawn:

1. Experiments revealed that the catalytic activity was maintained by means of catalyst regeneration processing despite the very large space velocity of the catalyst bed when the catalyst was used together with CaO at 1123 K.
2. Hydrogen concentrations of about 60 N_2-free vol%, which is almost the same as the equilibrium composition, and hydrogen production exceeding 50 mol/kg-feedstock were achieved at a gasification and reforming temperature of 1123 K.
3. The produced gas had a mean higher heating value in the range 6–10 MJ/m_N^3.
4. XRD analysis confirmed metallic nickel crystal growth when using the catalyst at 1123 K, despite repeated regeneration.

References

1. Sakoda A, Sadakata M, Koya T, Furusawa T, Kunii D (1981) Gasification of biomass in a fluidized bed. Chem Eng J 22: 221–227
2. van der Drift A, van Doorn J, Vermeulen JW (2001) Ten residual biomass fuels for circulating fluidized-bed gasification. Biomass Bioenergy 20:45–56
3. Piao G, Hendarsa AS, Adachi Y, Itaya Y, Hamai M, Mori S (2004) Research and development on high-temperature gasification technology of woody biomass for fuel cell power generation process (in Japanese). Kagaku Kogaku Ronbunshu 30:385–390
4. Fantozzi F, D'Alessandro B, Desideri U (2005) Integrated pyrolysis regenerated plant (IPRP) an efficient and scalable concept for gas turbine-based energy conversion from biomass and waste. J Eng Gas Turbines Power, Trans ASME 127:348–357
5. Wu W, Kawamoto K, Kuramochi H (2006) Hydrogen-rich synthesis gas production from waste wood via gasification and reforming technology for fuel cell application. J Mater Cycles Waste Manag 8:70–77
6. Asadullah M, Tomishige K, Fujimoto K (2001) A novel catalytic process for cellulose gasification to synthesis gas. Catal Commun 2:63–68
7. Swami SM, Abraham MA (2006) Integrated catalytic process for conversion of biomass to hydrogen. Energy Fuels 20:2616–2622
8. Furusawa T, Tsutsumi A (2005) Development of cobalt catalysts for the steam reforming of naphthalene as a model compound of tar derived from biomass gasification. Appl Catal A 278:195–205
9. Engelen K, Zhang Y, Draelants DJ, Baron GV (2003) A novel catalytic filter for tar removal from biomass gasification gas: improvement of the catalytic activity in presence of H_2S. Chem Eng Sci 58:665–670
10. Rapagna S, Jand N, Foscolo PU (1998) Catalytic gasification of biomass to produce hydrogen-rich gas. Int J Hydrogen Energy 23(7):551–557
11. Baker EG, Mudge LK, Brown MD (1987) Steam gasification of biomass with nickel secondary catalysts. Ind Eng Chem Res 26:1335–1339
12. Delgado J, Aznar MP, Corella J (1996) Calcined dolomite, magnesite, and calcite for cleaning hot gas from a fluidized bed biomass gasifier with steam: life and usefulness. Ind Eng Chem Res 35:3637–3643
13. Delgado J, Aznar MP (1997) Biomass gasification with steam in fluidized bed: effectiveness of CaO, MgO, and CaO–MgO for hot raw gas cleaning. Ind Eng Chem Res 36:1535–1543
14. Rapagna S, Jand N, Kiennemann A, Foscolo PU (2000) Steam-gasification of biomass in a fluidized-bed of olivine particles. Biomass Bioenergy 19:187–197